

## **A Comparative Study of Silver Screen Printing and Electroplating Metallization for High-Efficiency Silicon Solar Cells**

Asmaa BOUYELFANE<sup>1\*</sup> ; Mohammed BENRAMDANE<sup>2</sup>.

<sup>1,\*</sup> URMER Laboratory, Abou Bakr Belkaid University of Tlemcen, Algeria

<sup>2</sup> ETAP Laboratory, Department of Mechanical Engineering, faculty of technology, University of Tlemcen, Algeria

### **Abstract**

This study presents a comparative analysis of two silver-based metallization techniques for silicon solar cells: conventional silver screen printing and silver electroplating. Silver screen printing remains the prevailing industrial process because of its simplicity, scalability, and technological maturity, though its significant silver consumption contributes substantially to manufacturing costs. Recent advances in fine-line screen printing have reduced silver usage by forming narrower contact fingers with excellent electrical conductivity, thus maintaining high cell efficiency. Beyond a general process comparison, the study also investigates the geometry of the front metal grid, focusing on parameters such as finger width and height, and their impact on key electrical characteristics specifically the metal–semiconductor contact resistance, the finger line resistance, the series resistance, and ultimately the photovoltaic conversion efficiency of the cell.

In parallel, silver electroplating is examined as an alternative metallization route offering potential material cost reduction and improved control over contact dimensions and layer uniformity. However, this approach introduces new challenges related to process complexity, surface uniformity, and industrial integration, requiring further optimization.

Contour plots were used in the MATLAB simulations to show the evolution of efficiency as a function of two important variables. This method produced an efficiency gain of more than 2%. For validation, the simulation results were then contrasted with experimental data. Overall, the comparative analysis shows how grid geometry, electrical performance, and manufacturing cost are interdependent, highlighting the need for additional study to maximize both silver-based metallization methods for more effective and sustainable silicon solar cell production.

### **Keywords**

- Silver metallization, screen printing, electrodeposition, silicon solar cell, efficiency, contact resistance, sustainability

## 1. Introduction

A crucial stage in the production of silicon photovoltaic (PV) cells is metallization, which has a big impact on the cells' overall efficiency and electrical performance. In order to collect and transfer the photogenerated current with the least amount of resistive loss, metallization entails creating metal contacts on the silicon cells' surface.[1],[2],[3] Because of its exceptionally high electrical conductivity, chemical stability, and durability all of which are essential for optimizing the energy conversion efficiency of solar panels silver (Ag) is the preferred metal among those used. While silver's resistance to corrosion ensures the long-term stability of metal contacts under environmental stresses like temperature fluctuations, humidity, and UV exposure, its superior conductivity ensures effective current collection [1],[4].

Due to its ease of use, scalability, and affordability in large-scale manufacturing, screen printing of silver paste has been the standard method for metallization in silicon photovoltaic technology. This method creates the front-side grid that balances electrical performance and optical shading losses by printing a conductive silver pattern onto the cell surface and firing it.

However, due to the high cost of silver and its finite supply worldwide, screen printing usually necessitates a substantial amount of the metal. Additionally [5], the optimization of metallization geometry and paste formulation becomes more difficult as cell efficiencies increase and finger widths decrease.[6].

Alternative metallization techniques like electrodeposition have attracted a lot of attention lately. Benefits of electrodeposition include the ability to precisely control the thickness and shape of metal layers, the possibility of using less silver, and better electrical contact quality. Silver is electrochemically deposited onto predetermined areas of the silicon cell using this technique, which may result in more uniform and finer metal grids with reduced resistance and possibly improved mechanical robustness. In an effort to get around the drawbacks of either technique alone, electrodeposition also creates opportunities for hybrid processes that combine screen-printed contacts with a thin plated layer [10] [19].

Given the crucial role of metallization in dictating silicon solar cell performance and cost, a comparative study between conventional silver screen printing and emerging electrodeposition techniques is timely. Examining these technologies side-by-side allows evaluation of their impacts on electrical performance metrics such as contact resistivity, fill factor, and overall cell efficiency, as well as on manufacturing scalability, silver usage, and long-term durability. Such an analysis is essential to inform material and process selection that aligns with the photovoltaic industry's goals of achieving higher efficiencies, reducing material costs, and enhancing sustainability in large-scale solar power deployment.[11].

This article presents a detailed experimental comparison of silver metallization via screen printing and electrodeposition on silicon solar cells. It discusses the methodologies, evaluates performance outcomes, and addresses technological challenges and prospects, aiming toward advancing high-efficiency silicon PV technologies.

If desired, the introduction can be further adapted, for example to emphasize environmental aspects related to silver resource constraints or industrial scaling challenges. Let me know if a more technical or more general tone is preferred.

### **1.1. Silver Screen Printing Metallization**

A commercially prepared silver paste made of fine silver particles (average diameter  $\sim$ 1  $\mu\text{m}$ ), glass frit binders, and organic solvents specifically designed for silicon solar cells was used for the screen printing metallization. A 325 mesh stainless steel screen with predefined finger widths of about 40  $\mu\text{m}$  was used for printing. In order to maximize the trade-off between optical shading and electrical conduction, the silver grid pattern had three busbars and twelve primary fingers. Before being fired in a belt furnace with peak temperatures ranging from 750 to 850  $^{\circ}\text{C}$ , the printed films were dried at 150  $^{\circ}\text{C}$  for ten minutes. This allowed the silver particles to sinter to the silicon surface and form ohmic contacts. To achieve uniform deposition and reduce defects, process parameters like paste viscosity, squeegee pressure, and print speed were optimized [2],[3].

### **1.2. Electrodeposition Metallization**

In order to control deposit morphology, stabilizing agents and surfactants were added to an aqueous silver nitrate-based electrolyte bath used for silver electrodeposition. The bath was kept at 25  $^{\circ}\text{C}$  and contained 0.05 M  $\text{AgNO}_3$  and 0.1 M potassium nitrate as an electrolyte support. For 30 seconds per cell, electrochemical deposition was performed under potentiostatic control at a steady voltage of 0.3 V vs.  $\text{Ag}/\text{AgCl}$  reference electrode. Cell surfaces were cleaned and masked to identify the metallization areas that matched the screen-printed patterns before deposition. To enhance layer adhesion and electrical contact quality, the samples were rinsed, dried, and then mildly annealed for five minutes at 200  $^{\circ}\text{C}$ . The silver layers that were deposited usually had fine-grained microstructures and thicknesses of 10–20  $\mu\text{m}$ . [6], [7] [19].

### **1.3. Cost Analysis**

Screen printing consumes 10-15 mg/W Ag (50-150 mg/M2 cell) via thick paste, driving metallization costs to 0.14-0.28  $\text{¥}/\text{Wp}$  (40-50% of cell processing), highly volatile with Ag prices (\$20-50/oz). Electroplating slashes Ag to 1-1.1 mg/W (1-9 mg/cell) as a thin cap over Ni seed, reducing costs by 40-60% to 0.08-0.11  $\text{¥}/\text{Wp}$  despite higher capex (payback 1-2 years), enabling  $<1$  mg/W targets for PERC/TOPCon. [4], [15] ,[18].

### **1.4. Industrial Performance**

Both achieve  $>22\%$  efficiencies in PERC cells, but electroplating enables finer grids (5-30  $\mu\text{m}$  fingers vs. 30-50  $\mu\text{m}$ ), cutting shading losses (3-5% absolute gain) and series resistance, boosting FF by 1-2% at optimal spacings (1.5-2.5 mm). Screen printing dominates 95% market share (high throughput,  $>5000$  wafers/h) but faces Ag limits (240 GW PV demand); electroplating scales to 3000-4000 wafers/h with seed printing + plating lines, already industrial at Meyer Burger/REC. [16].

### 1.5. Lifecycle Reliability

Both meet 25-30 year warranties (<0.5-0.8%/yr degradation, IEC 61215), with screen printing showing 5-7% damp heat loss (1000h 85°C/85% RH) from firing cracks/Ag migration, versus electroplating's <5% loss due to ductile Ni/Ag layers and reduced stress. Field data confirms equivalent Voc/FF stability in EVA/POE encapsulants.

Parameter	Ag Screen Printing	Ag Electroplating	Advantage
Ag Consumption (mg/W)	10-15	1-1.1	Electroplating (90%↓)
Cost (¥/Wp)	0.14-0.28	0.08-0.11	Electroplating (50%↓)
Efficiency (PERC)	22-23%	23-24%	Electroplating
Throughput (wph)	>5000	3000-4000	Screen Printing
Damp Heat Loss (1000h)	5-7%	<5%	Electroplating

**Table 1** Comparative Performance Metrics of Ag Screen Printing vs. Ag Electroplating Metallization in Silicon Solar Cells [15] [16].

When it comes to cost-performance-reliability trade-offs, electroplating is superior because it reduces Ag dependency while matching industrial maturity, which is crucial for gigawatt-scale PV in the face of resource constraints.

## 2. Methodology

Although screen printing is the most widely used contacting method for silicon solar cells, few studies were available to study the nature of the contact. Recent efforts by some European research groups lead to a convincing model of contact formation [8].

### 2.1. Series resistance

Series resistance in a solar cell has three causes: firstly, the movement of current through the emitter and base of the solar cell; secondly, the contact resistance between the metal contact and the silicon; and finally the resistance of the top and rear metal contacts. The main impact of series resistance is to reduce the fill factor, although excessively high values may also reduce the short-circuit current [9], [17].

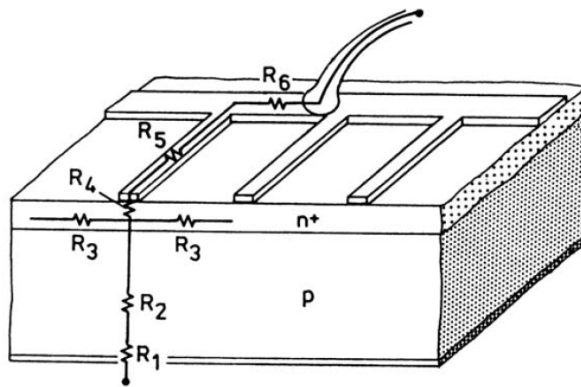


**Fig 1:** Series resistance in a solar cell [7].

The individual resistances are:

R1: The metal-semiconductor-contact on total back surface,

R2: The semiconductor material (base),

R3: The emitter between two grid fingers,

R4: The metal-semiconductor-contact on the grid finger,

R5: The grid finger, and

R6: The collection bus.

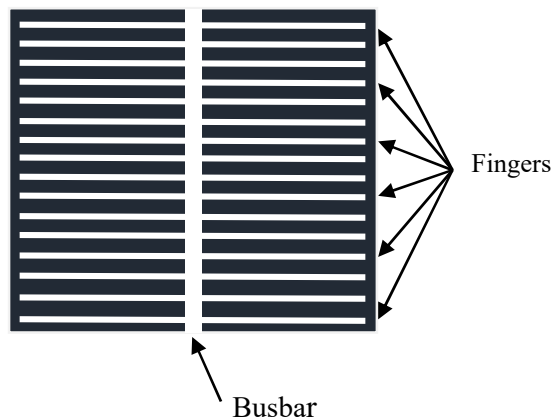


**Fig 2:** Top contact design in a solar cell. The busbar connect the fingers together and pass the generated current to the external electrical contacts [13].

The finger width  $w_f$  of the plated contact is equal to the sum of twice the plating height  $h_f$  and the contact width  $w_c$  [13].

$$w_f(h_f) = 2 h_f + w_c \quad (1)$$

The cross section area  $A_f$  of the plated finger can be calculated by:

$$A_f(h_f) = w_c \cdot h_f + \frac{1}{2} \cdot \pi \cdot (h_f)^2 \quad (2)$$

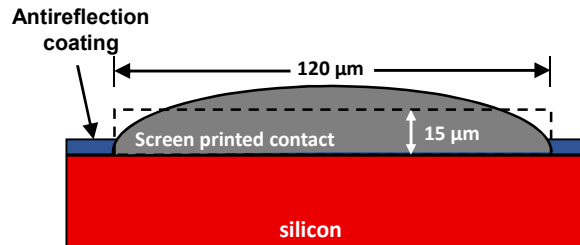


Fig.3. A screen-printed contact finger. [17]

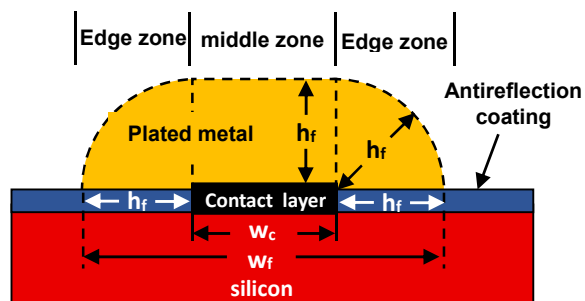


Fig. 4. Assumed contact geometry for a plated. [17]

Common Parameters screen printed and plated front side contacts			
<b>L</b>	length cell	<b>p</b>	Number of busbar
<b>w<sub>bus</sub></b>	width busbar	<b>d</b>	finger separation distance
<b>m</b>	number soldering joints	<b>R<sub>sh</sub></b>	sheet resistance emitter
<b>ρ<sub>b</sub></b>	base resistivity	<b>ρ'<sub>m</sub></b>	resistivity metal rear side
<b>e</b>	thickness of the base	<b>ρ'<sub>c</sub></b>	contact resistivity rear side
<b>h'</b>	height metal rear side		
<b>Parameters of screen printed contact</b>		<b>Parameters of plated contact</b>	
		<b>w<sub>c</sub></b>	width contact layer
<b>w<sub>s</sub></b>	width screen-printed contact	<b>w<sub>f</sub></b>	total contact width
<b>(h<sub>bus</sub>)<sub>s</sub></b>	height of screen-printed busbar	<b>h<sub>bus</sub></b>	height plated busbar
<b>h<sub>s</sub></b>	height of screen-printed contact	<b>h<sub>f</sub></b>	height plated contact
<b>(ρ<sub>c</sub>)<sub>s</sub></b>	contact resistivity screen-printed grid	<b>ρ<sub>c</sub></b>	contact resistivity (front)
<b>ρ<sub>s</sub></b>	resistivity screen-printed silver	<b>ρ<sub>m</sub></b>	resistivity plated metal

Table 2 Definition of symbols used for loss calculation and parameters describing the grid pattern[17]

Resistance	Cells with screen-printed contacts ( $\Omega$ )	Cells with plated contacts ( $\Omega$ )
Emitter	$\frac{R_{sh}d^2}{12L^2}$	idem
Finger	$\frac{d\rho_s}{12h_s w_s p^2}$	$\frac{d\rho_m}{12p^2 \left( h_f w_c + \frac{\pi h_f^2}{2} \right)}$
busbar	$\frac{\rho_s d^2}{6pL(h_{bus})_s w_{bus}} \left( \frac{L^2}{2m^2 d^2} + 3 \frac{L}{2md} + 1 \right)$	$\frac{\rho_m d^2}{6pLh_{bus} w_{bus}} \left( \frac{L^2}{2m^2 d^2} + 3 \frac{L}{2md} + 1 \right)$
front contact	$\frac{d\sqrt{(\rho_c)_s R_{sh}}}{2L^2} \coth \left( \frac{w_s}{2} \sqrt{\frac{R_{sh}}{(\rho_c)_s}} \right)$	$\frac{d\sqrt{\rho_c R_{sh}}}{2L^2} \coth \left( \frac{w_c}{2} \sqrt{\frac{R_{sh}}{\rho_c}} \right)$
Base	$\frac{e\rho_b}{L^2}$	idem
Metal layer rear side	$\frac{\rho'_m h'}{L^2}$	idem
rear contact	$\frac{\rho'_c}{L^2}$	idem
shading fraction	$\frac{1}{d} \left( w_s + \frac{pw_{bus}(d - w_s)}{L} \right)$	$\frac{1}{d} \left( w_c + 2h_f + \frac{pw_{bus}(d - w_c - 2h_f)}{L} \right)$

**Table 3:** Resistive contributions of a solar cell and the recovery rate [14]. For definition of symbols [17]

## 2.2. Shadowing Losses by Contact Fingers

Shading losses are caused by the presence of metal on the top surface of the solar cell which stops light from entering the solar cell. The shading losses are determined by the transparency of the top surface, which, for a planar top surface, is defined as the fraction of the top surface covered by metal. The transparency is determined by the width of the metal lines on the surface and on the spacing of the metal lines [3]. An important practical limitation is the minimum line-width associated to a particular metallization technology. For identical transparencies, a narrow line-width technology can achieve closer finger spacing, thus reducing the emitter resistance losses [9].

The power loss resulting from shadowing of the semiconductor by the grid lines and busbar is [6].

$$P_{shadow} = P_L \eta n (aw + 2bw') \quad (3)$$

### 2.3. Grid optimization for maximum power point:

Assuming no power loss the maximum power output  $P_{mpp,max}$  would be equal to:

$$P_{mpp,max} = V_m I_m = V_m j_m L^2 \quad (4)$$

Resistive losses are the sum of different contributions listed in Table 2. The total power dissipated  $P_t$  due to resistive losses and shading fraction is expressed by the equation (4).

$$P_t = P_r + P_o = I_m^2 \Sigma r + F I_m V_m = j_m^2 L^4 \Sigma r + F j_m V_m L^2 \quad (5)$$

With

$P_t$ : total power dissipated in W

$P_r$ : dissipated power due to the contributions of series resistance in W

$P_o$ : dissipated power due to the shading fraction in W

$\Sigma r$  : sum of all resistance contributions of table 2 in  $\Omega$ .

From this relation, it is possible to calculate the total loss fraction in % given by the equation 5. The optimal geometric parameters for which this loss factor is minimal can then be determined.

$$\text{total losses} = \frac{P_t}{V_m I_m} = \frac{P_t}{V_m j_m L^2} \quad (6)$$

Hence the power at maximum power point can be calculated by:

$$P_{mpp} = V_{mpp} I_{mpp} = V_{mpp} j_{mpp} L^2 \quad (7)$$

$$P_{mpp} = \frac{(P_{mpp,max} - P_t)}{L^2} \quad (8)$$

Fill factor is defined as the ratio of the maximum power output of a solar cell to the product of its open-circuit voltage and short-circuit current. The fill factor (FF) for a cell can be written as:

$$FF = \frac{P_{mpp}}{V_{oc} I_{sc}} = \frac{V_{mpp} I_{mpp}}{V_{oc} I_{sc}} \quad (9)$$

The efficiency of a solar cell is defined as the ratio of the photovoltaically generated electric output of the cell to the luminous power falling on it:

$$\eta = \frac{V_{mpp} I_{mpp}}{P_{light}} = \frac{FF V_{oc} I_{sc}}{P_{light}} \quad (10)$$

### 3. Results and Discussion

We model and simulate the different contributions to the series resistance and the shade rate for an Ag electroplated contact and compare the outcomes with those of a traditional screen-printed front side silver contact. In this work, a mathematical model that enables the analysis of the impact of optical and electrical losses on solar cell efficiency by creating a set of variations of the dominating parameters in the structure of the front side collecting grid is implemented using the MATLAB environment.

We chose a grid with two 2 mm wide busbars with a height of 15 mm for industrial solar cell (area  $12,5 \times 12,5 \text{ cm}^2$ ), on a  $40 \Omega/\text{sq}$  emitter sheet resistance, for a short-circuit current density  $J_{sc}$  equal to  $35 \text{ mA/cm}^2$ . The finger width in the case of screen-printing is limited by technological constraints ( $w_f > 100 \mu\text{m}$ ). Generally, fingers  $120 \mu\text{m}$  wide are used in commercial cells, and that's the width we used in this study, while much thinner line contacts can be made by electrochemical deposition, width contact layer  $w_c = 30 \mu\text{m}$  and height of 15mm which makes a total contact width  $w_f = 60 \mu\text{m}$ .

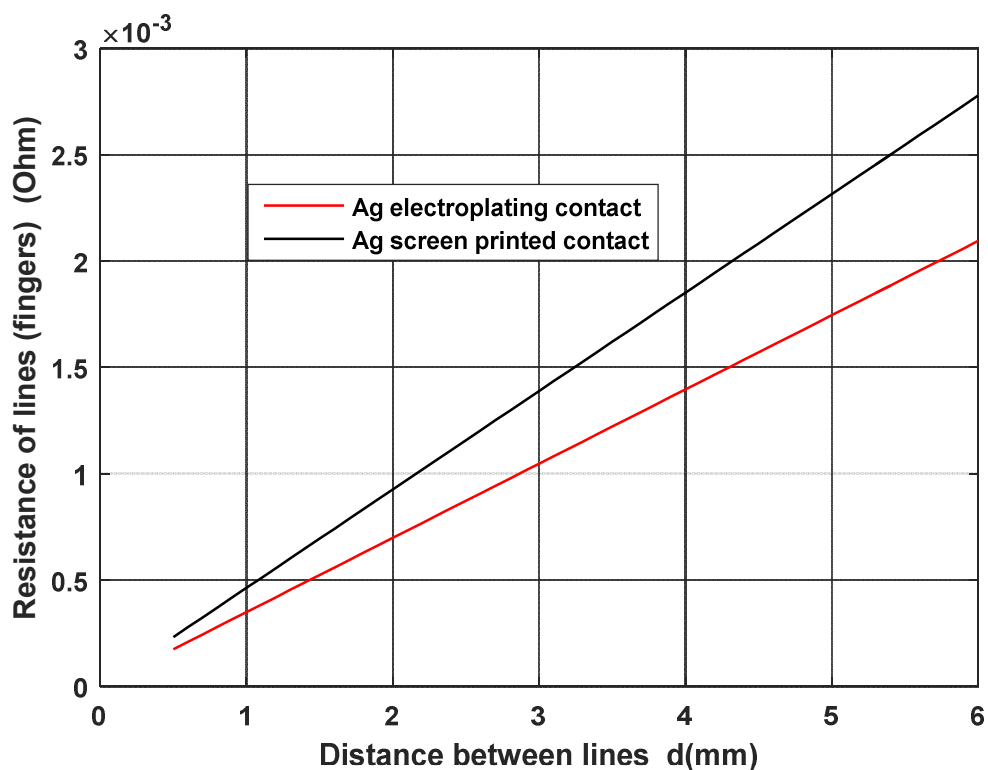


**Fig. 5.** Resistance of lines as a function of distance between fingers.

The evolution of the finger line resistance for two silver-based front metallization technologies Ag screen printed contacts and Ag electroplated contacts as a function of the distance between fingers is depicted in the figure. Because of the longer current path in the fingers and the corresponding increase in ohmic losses, the resistance for both technologies increases nearly linearly with increasing finger spacing. Better electrical conduction and a smaller contribution to the total series resistance of the solar cell are indicated by the Ag electroplated fingers' lower resistance at any given spacing compared to the Ag screen printed fingers. This finding implies that electroplated Ag metallization provides a benefit for reducing

resistive losses, especially when front-side shading is minimized by using larger finger spacings.

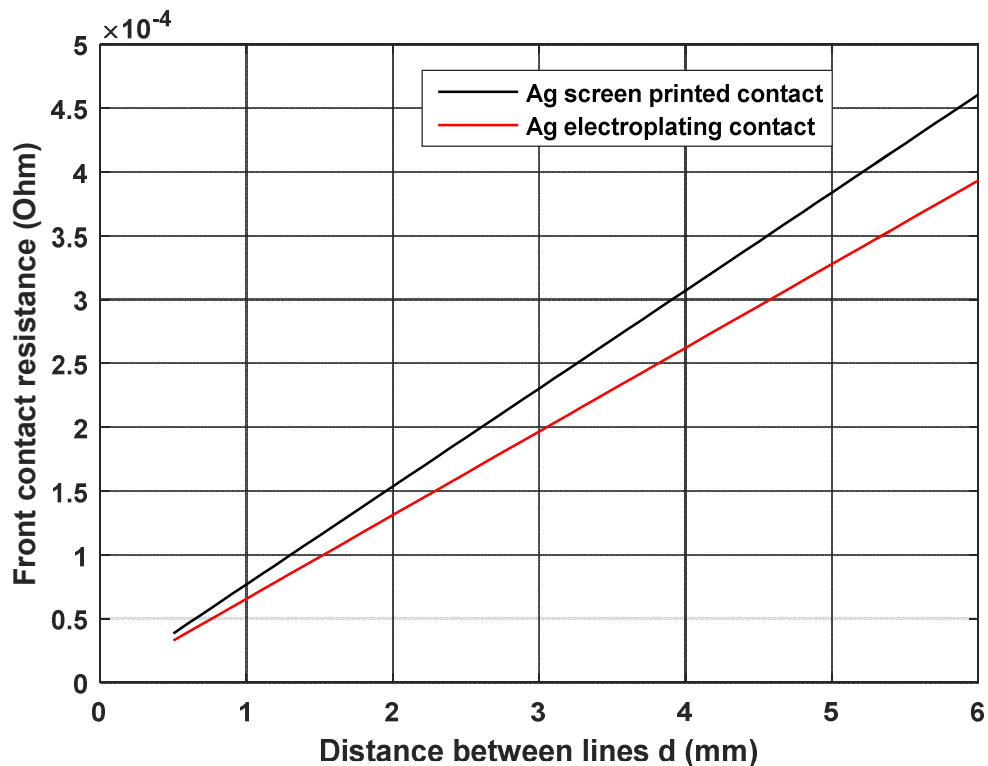


**Fig.6.** Front contact resistance as a function of distance between fingers.

The front contact resistance variation for two silver-based metallization technologies Ag screen printed and Ag electroplated contacts as a function of finger separation is shown in the figure. Due to the longer lateral transport path of carriers in the emitter before they reach a metal finger and the consequent increase in ohmic losses, the front contact resistance for both technologies increases nearly linearly with increasing finger spacing. Better contact quality and a smaller contribution to the total series resistance are indicated by the Ag electroplated contact's lower front contact resistance at any given spacing compared to the Ag screen printed contact. Ag electroplating is more advantageous for reducing resistive losses at the metal–semiconductor interface, especially when larger finger. This behavior confirms that Ag electroplating is more favorable for minimizing resistive losses at the metal–semiconductor interface, particularly when larger finger spacings are adopted to reduce front-side shading.

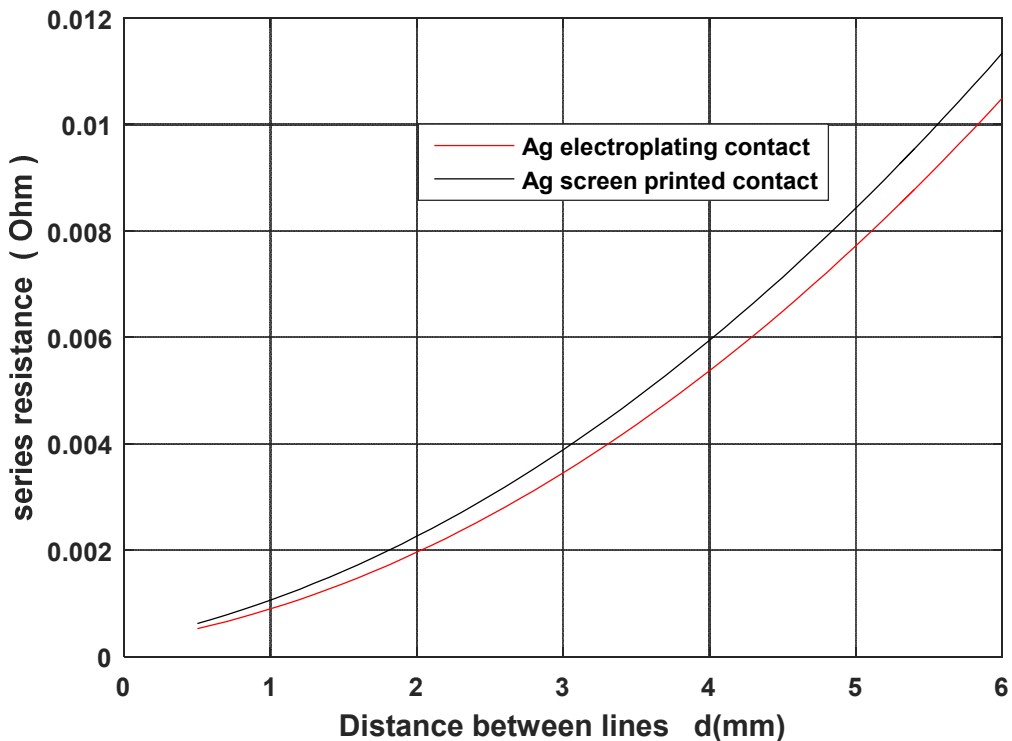


**Fig. 7.** Series resistance as a function of distance between fingers.

For both Ag screen-printed and Ag electroplated contacts, Figure 7 shows the evolution of the series resistance related to the front metal fingers as a function of the distance between adjacent fingers. For both technologies, the resistance of the fingers increases nearly linearly as  $d$  increases, reflecting the longer current path and consequent enhancement of ohmic losses in the grid and emitter region. However, the Ag electroplated fingers consistently show a lower resistance than the Ag screen-printed ones for any given spacing, suggesting a lower line resistance and, consequently, a smaller contribution to the solar cell's overall series resistance. This behavior implies that, particularly when larger finger spacings are needed, electroplated Ag metallization is more advantageous for reducing resistive losses.

This conduct implies that screen-printed contacts are more sensitive to spacing optimization to prevent negative effects on fill factor and cell efficiency, whereas electroplated Ag metallization is more advantageous for minimizing resistive losses, particularly when larger finger spacings are needed to limit optical shading.

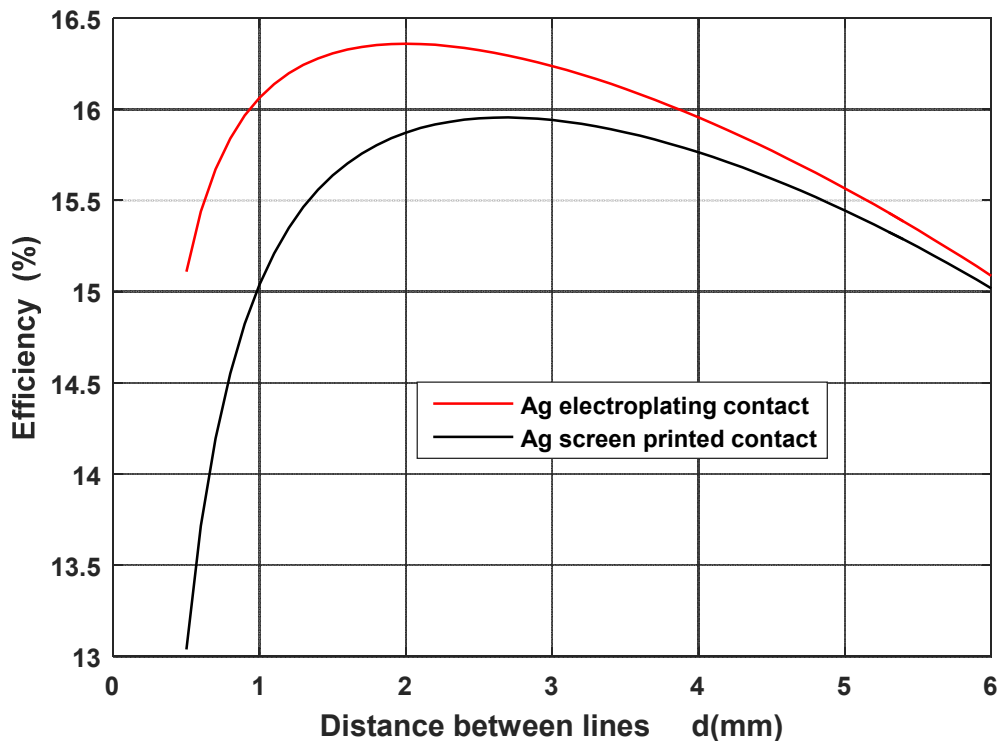


**Fig. 8.** Efficiency as a function of distance between fingers.

Figure 8 shows the variation of solar cell efficiency as a function of the distance between front metal fingers ( $d$ ), typically comparing Ag screen-printed and Ag electroplated metallization technologies in silicon photovoltaic cells. Efficiency initially increases with larger finger spacing due to reduced shading losses, which allow more light absorption, but eventually decreases as spacing becomes excessive, leading to higher lateral carrier transport resistance in the emitter and increased series resistance losses.

Both metallization types exhibit an optimal spacing where efficiency peaks, often around 1.5-2.5 mm depending on finger width and cell design, balancing optical gains against electrical losses. Ag electroplated contacts generally achieve higher peak efficiencies than screen-printed ones at equivalent spacings, thanks to lower finger resistance and better contact resistivity, enabling wider spacing without severe efficiency drops.

This behavior underscores the need for grid geometry optimization in metallization: narrower, taller fingers from electroplating reduce silver use while minimizing shading (down to 5-30  $\mu\text{m}$  widths) and resistive penalties, supporting efficiencies over 20-22% in PERC or advanced cells. In this comparative study, Fig. 8 highlights electroplating's superiority for low-shading designs, directly impacting fill factor and overall cell performance.

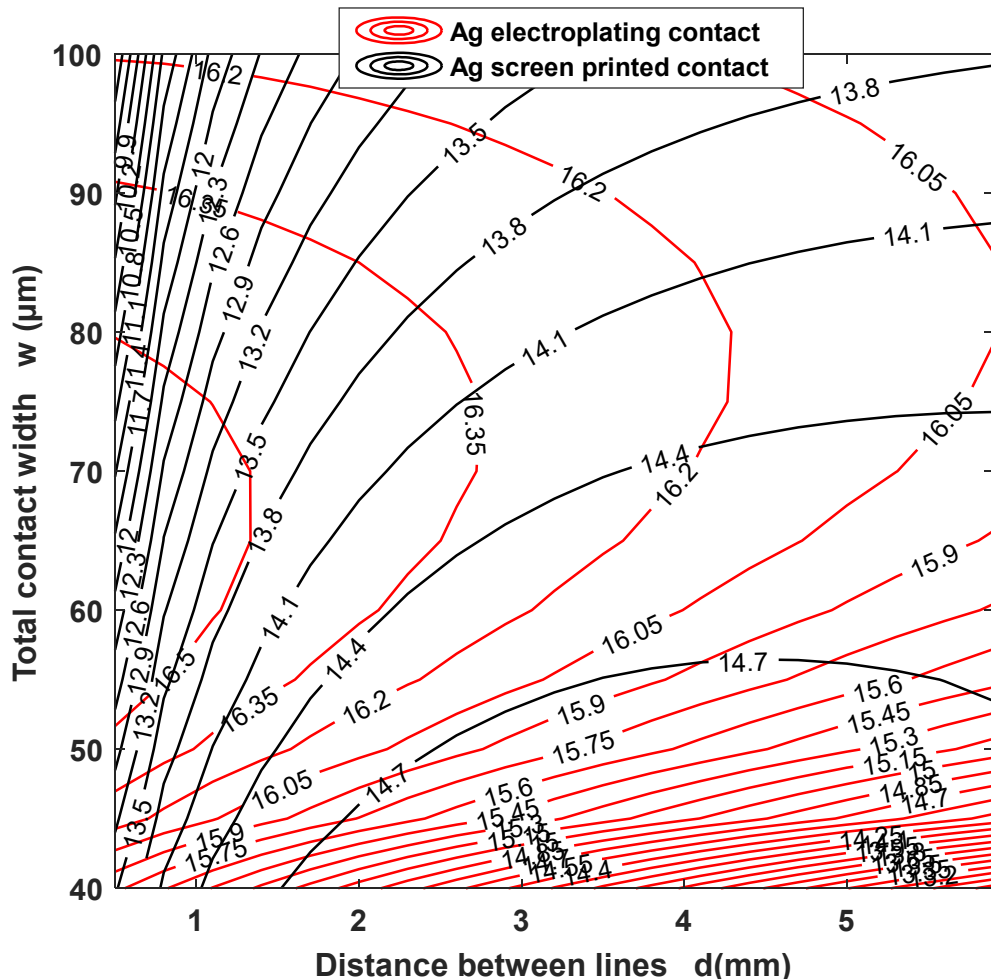


**Fig. 9.** Contours represent the solar cell efficiency as a function of distance between fingers and the total contact width.

Fig. 9 displays contour lines representing solar cell efficiency as a function of two key front metallization parameters: the distance between fingers (finger spacing) and the total contact width. These contours reveal optimal trade-offs between optical shading losses and resistive (ohmic) losses in the emitter. Contour lines connect points of constant efficiency, with denser central regions indicating the efficiency peak. Increasing finger spacing reduces shading but raises lateral current flow resistance in the emitter; wider total contact lowers series resistance but increases shading. The optimal zone typically centers around 1-2 mm spacing and metal-specific widths

## Conclusion

This study compared the metallization processes of electroplating and silver-based screen printing, with an emphasis on line resistance, contact resistance, and total series resistance. The findings show that, in comparison to traditional screen printing, the electroplating method significantly reduces line and contact resistances, resulting in a lower

total series resistance. As a result, electroplated solar cells have higher fill factor and conversion efficiency.

Economically speaking, electroplating offers significant reductions in silver consumption, which lowers material costs and improves manufacturing sustainability, even though it necessitates more sophisticated equipment and initial process control. On the other hand, despite its higher resistive losses, screen printing is still beneficial due to its ease of use and high throughput.

Overall, the results indicate that electroplating shows promise as a low-cost, high-efficiency alternative for the production of next-generation solar cells, particularly as the industry moves toward finer front-grid architectures and thinner wafers.

## References

- [1] **Sebastian Tepner and Andreas Lorenz** “Printing technologies for silicon solar cell metallization: A comprehensive review” Progress in PHOTOVOLTAIC Volume31, Issue6 June 2023 Pages 557-590
- [2] **Andreas Lorenz , Michael Linse , Herbert Frintrup , Martin Jeitler , A. Mette , M. Lehner , R. Greutmann , H. Brocker** , “screen printed thick film metallization of silicon solar cells - recent developments and future perspectives” Presented at the 35th European PV Solar Energy Conference and Exhibition, 24-28 September 2018, Brussels, Belgium
- [3] **Karim Abdel Aal, Norbert Willenbacher** “Front side metallization of silicon solar cells A high-speed video imaging analysis of the screen printing process” Solar Energy Materials and Solar Cells Volume 217, November 2020, 110721
- [4] **Mark Thirsk, Linx Consulting LLC, Mendon, Massachusetts** “Progress in cost reduction in silver pastes for crystalline silicon cells” Photovoltaics International 2011 <https://www.pv-tech.org/>
- [5] **Hariklia (Lili) Deligianni, Shafaat Ahmed, and Lubomyr T. Romankiw** “ The Next Frontier: Electrodeposition for Solar Cell Fabrication” The Electrochemical Society Interface • Summer 2011
- [6] **Atteq ur Rehman , Soo Hong Lee** “Review of the Potential of the Ni/Cu Plating Technique for Crystalline Silicon Solar Cells” Materials (Basel). 2014 Feb 18;7(2):1318–1341. doi: 10.3390/ma7021318 Review of the Potential of the Ni/Cu Plating Tec
- [7] **J.-D.Lee,etal.,RenewableEnergy(2011)**, <http://dx.doi.org/10.1016/j.renene.2011.10.007>.
- [8] **Vikrant A. Chaudhari, Chetan S. Solanki**, Two Step Ni/Cu Metallization for Commercial c-Si Solar Cells: 1 to 10 Suns, IEEE 978-1-4244- 5892-9/10/\$26.00, 2010
- [9] **J.Bartsch, A. Mondon,C. Schetter, M. Hörteis, S.W.Glunz.** Copper as conducting layer in the front side metallization of crystalline silicon solar cells challenges, processes and

characterization, in: Proceeding of the Second Workshop on Metallization, Constance, Germany, 2010.

[10] **Mugdesem Tanrioven** Photovoltaic Systems Engineering for Students and Professionals First edition published 2024 by CRC Press

[11] **DIETER K. SCHRODER** Semiconductormaterial And Device Characterization Third Edition A JOHN WILEY & SONS, INC., PUBLICATION 2006

[12] **Antonio Luque and Steven Hegedus** Handbook of Photovoltaic Science and Engineering John Wiley & Sons Ltd, Copyright 2003

[13] **A. Mette**, New Concepts for Front Side Metallization of Industrial Silicon Solar Cells, Fraunhofer-Institut für Solare Energie systeme Freiburg im Breisgau, 2007 (Ph.D. Thesis).

[14] **C. Boulord**, Développement de techniques de métallisation innovantes pour cellules photovoltaïques à haut rendement, Ph.D. Thesis, INSA Lyon, 2011.

[15] **Yuchao Zhang , Sisi Wang , Li Wang , YuanChih Chang , Ran Chen** , Silver-lean screen-printing metallisation for industrial TOPCon solar cells: Enabling an 80 % reduction in silver consumption Solar Energy Materials and Solar Cells Volume 288, 15 August 2025,

[16] **Steffen Schuler & Ilka Luck** Cell metallization by screen printing: Cost, limits and alternatives PICON Solar GmbH, Berlin, Germany

[17] **A.Bouyelfane , A.Zerga** Ni/Cu electroplating, a worthwhile alternative to use instead of Ag screen-printed front side metallization of conventional solar cells MaterialsScienceinSemiconductorProcessing26(2014)312–319

[18] **Zhang Y. et al.**, “Roadmap towards 1 mg/W Silver Consumption for Industrial High-Efficiency Silicon Solar Cells”, APVI Solar Research Conference, 2023.

[19] **Yuan-Chih Chang, Yuchao Zhang, Li Wang, Sisi Wang, Haoran Wang, Chien-Yu Huang, Ran Chen, Catherine Chan, Brett Hallam** Silver-lean metallization and hybrid contacts via plating on screen-printed metal for silicon solar cells manufacturing Progress in PHOTOVOLTAIC Volume33, Issue1 EU PVSEC 2023 January 2025 Pages 158-169